# Modeling and Stress–Strain Characteristics of the Mechanical Properties of Carbon-Nanotube-Reinforced Poly(vinyl acetate) Nanocomposites

**Remo Merijs Meri,[1] Juris Bitenieks,[1] Martins Kalnins,[1] Robert Maksimov[2]**

[1]*Institute of Polymer Materials, Riga Technical University, 14/24 Azenes Street, Riga, LV-1048, Latvia*
[2]*Institute of Polymer Mechanics, University of Latvia, 23 Aizkraukles Street, Riga, LV-1006, Latvia*

Received 28 April 2011; accepted 28 April 2011
DOI 10.1002/app.34767
Published online 10 August 2011 in Wiley Online Library (wileyonlinelibrary.com).

**ABSTRACT:** Polymer/carbon nanotube (CNT) composites are one of the most perspective advanced materials developed in recent years. The properties of CNT-reinforced polymer composites, however, strongly depend on structural aspects of the nanostructured filler and on its dispersion quality in a polymer matrix. Consequently, this research was devoted to the investigation of multiwalled-CNT-modified poly(vinyl acetate) (PVAc) composites with respect to the mechanical property dependence on some structural characteristics of CNTs. PVAc/CNT nanocomposites were obtained with a solution casting technique. The amount of CNTs was changed from 0.01 up to 2 wt %. The stress–strain characteristics of PVAc/CNT nanocomposites clearly revealed remarkable reinforcing effects of the CNT additions already at 0.01 wt %. At this CNT concentration, the elastic modulus ($E$) and tensile yield stress increased by 12.5 and 60%, respectively. Special attention was paid to the change of $E$ with respect to some structural characteristics of CNTs. A corresponding mathematical model for the prediction of the elastic properties of CNT polymer nanocomposites is proposed, showing that elastic constants of the nanocomposites largely depend on the agglomeration of CNTs. © 2011 Wiley Periodicals, Inc. J Appl Polym Sci 122: 3569–3573, 2011

**Key words:** strain; stress; modeling

## INTRODUCTION

Carbon nanotubes (CNTs), since their discovery in 1991, have attracted considerable interest of scientists because of their unique electrical, thermophysical, mechanical, and other properties. Multiple studies have been devoted to the structural, processing, mechanical, and other issues[1–20] of CNT-modified polymer nanocomposites. For example, a considerable increment in the elastic modulus ($E$) of CNT-containing poly(vinyl alcohol) composites (1.5 times and 10 times below and the above glass-transition temperature, respectively) was reported by Shaffer and Windle,[4] who considered that the regular dispersion of the nanofiller was ensured and agglomeration was prevented. Considerable increments of the indicators of the mechanical properties of CNT-reinforced polymer nanocomposites were also reported by other authors.[14–20] The effect of small additions of multiwalled CNTs on the indicators of the structural, calorimetric, thermogravimetric, and electric properties of poly(vinyl acetate) (PVAc) matrix nanocomposites was also demonstrated in our previous research.[6] It should be noted, however, that experimental values of the indicators of mechanical properties of polymer composites based on CNTs have proven to be significantly lower than those predicted theoretically with the methods of the mechanics of composite continuous media.[7–9]

Microphotographs obtained by transmission electron microscopy, presented in some studies,[10–13] have demonstrated the great diversity of the structure of CNT-based composites. Even at a rather good dispersion, the nanotubes, as a rule, have a random orientation and are strongly curved, with a curvature that varies along their length. With increased concentration of CNTs, entangled fibrous agglomerates in the form of disorderly crimped nanotube clusters arise. The complicated geometry of CNTs in a composite, on the one hand, inevitably reduces the efficiency of the reinforcement of materials and, on the other hand, considerably complicates the theoretical modeling of the composite properties.

This research was devoted to the investigation of the mechanical properties of CNT-modified PVAc nanocomposites and the fitting of a mathematical model for the prediction of its elastic characteristics.

## EXPERIMENTAL

Finndisp HW 1 PVAc, with a glass-transition temperature of 22.5°C, was used as a thermoplastic

*Correspondence to:* R. Maksimov (maksimov@edi.lv).

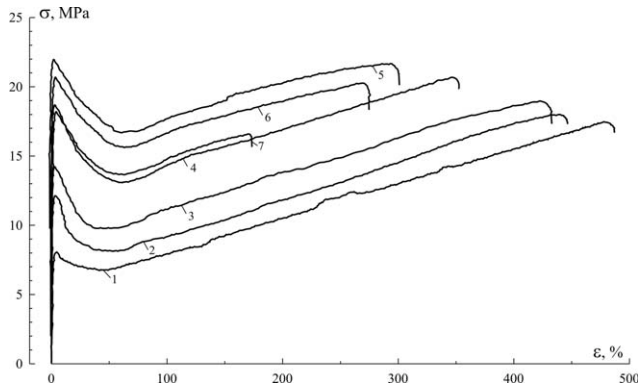


**Figure 1** Stress (σ)–strain (ε) diagrams of the (1) unfilled PVAc and PVAc/CNT nanocomposites at the following $W_f$ values: (2) 0.01, (3) 0.05, (4) 0.1, (5) 0.5, (6) 1, and (7) 2 wt %.

matrix, whereas Bayer Baytubes (CNTs) were used as a nanostructured filler for manufacturing the nanocomposites by a solution casting method. The concentration of the CNTs in PVAc was varied from 0.01 to 2 wt %. Sodium dodecyl sulfate was used as a stabilizing agent in the PVAc/CNT water dispersions.

The tensile stress–strain characteristics of PVAc/CNT nanocomposites at 23 ± 2°C were determined according to ISO 527 with a Zwick/Roell BDO020 universal testing machine (Zwick GmbH & Co. KG, Ulm, Germany). Before testing, all of the specimens were conditioned in an exicator above silica gel until their weight was stabilized.

## RESULTS AND DISCUSSION

In the beginning, let us turn to the experimental results of the PVAc/CNT composites. The stress–strain diagrams of the unfilled PVAc and its composites with CNTs are shown in Figure 1. As one can see, the stress–strain diagrams of the PVAc/CNT nanocomposites were shifted to higher stress and lower strain values in comparison to those of the neat polymer. All of the specimens deformed by showing smooth yield maxima followed by strain hardening. It is important to mention that the rate of strain hardening was approximately the same for all of the investigated nanocomposites.

The stress–strain characteristics of the PVAc/CNT nanocomposites as functions of the nanofiller weight content ($W_f$) are shown in Figure 2. As one can see, $E$, yield stress ($\sigma_y$), and stress at break ($\sigma_b$) increased to certain maximum values in the interval of CNT concentrations investigated. The elongation at break ($\varepsilon_b$) of the investigated nanocomposites at the same $W_f$ values decreased from more than 500 to 200%. With increasing nanotube concentration above 0.5%, the gain in $E$ slowed down, whereas the values of $\sigma_y$ and $\sigma_b$ even decreased. To explain this behavior, a detailed analysis of the elastic constants of the PVAc/CNT nanocomposites is presented next.

According to a known generalized Eshelby solution[21] for a composite containing a small concentration of uniaxially oriented [one-dimensional (1D)] ellipsoidal inclusions, the elasticity tensor ($\mathbf{C^*}$) can be expressed as follows:

$$\mathbf{C}^* = \mathbf{C^m} + V_f(\mathbf{C^f} - \mathbf{C^m})\mathbf{A^f} \text{ and } \mathbf{A^f} = A_{dilute} = \left[\mathbf{I} + \mathbf{S}(\mathbf{C^f} - \mathbf{C^m})(\mathbf{C^m})^{-1}\right]^{-1} \quad (1)$$

where $V_f$ is the volume fraction of inclusions; $\mathbf{C^f}$ and $\mathbf{C^m}$ are the rigidity tensors of the inclusion and matrix, respectively; $A_{dilute}$ is the strain concentration tensor according to Eshelby; $\mathbf{S}$ is the Eshelby tensor;[21] $\mathbf{I}$ is the fourth-rank unit tensor with the components $\mathbf{I}_{ijkl} = 1/2(\delta_{ik}\delta_{jl} + \delta_{ik}\delta_{jk})$, where $\delta_{ik}$ is the Kronecker δ and $\mathbf{A^f}$ is the strain concentration tensor.

In the case of a finite concentration of a nanofiller and with consideration of its elastic interaction in the composite, the Mori–Tanaka model[22] is applicable, according to which the tensor has the form

$$A^{\mathbf{f}} = A_{MT} = A_{dilute}\left[(1 - V_f)\, I + V_f A_{dilute}\right]^{-1} \quad (2)$$

where $A_{MT}$ and $A_{dilute}$ are strain concentration tensors according to Mori-Tanaka and Eshelby, respectively. Analytical equations for calculations of the elasticity constants of composites [tensile $E$, shear modulus, and Poisson's ratio (ν)] with uniaxially and randomly oriented {both spatially [three-dimensional (3D)] and planary [two-dimensional (2D)]} ellipsoidal inclusions are presented in refs. 23 and 24.

In Figure 3, the experimental values of $E$ of various compositions of the PVAc/CNT nanocomposites are compared with theoretically calculated values for 1D, 2D, and 3D orientations of the nanofiller. In the calculations, we assumed that $E$, ν, and the aspect ratio of the CNTs were $E_f$ = 900 GPa, $\upsilon_f$ = 0.25, and $l/d_f$ = 200, respectively, whereas $E$ and

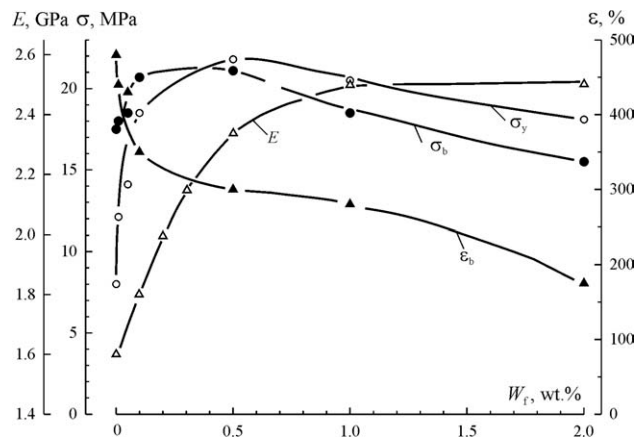


**Figure 2** Experimental values of $\sigma_y$, $\sigma_b$, $\varepsilon_b$, and tensile $E$ as functions of $W_f$.

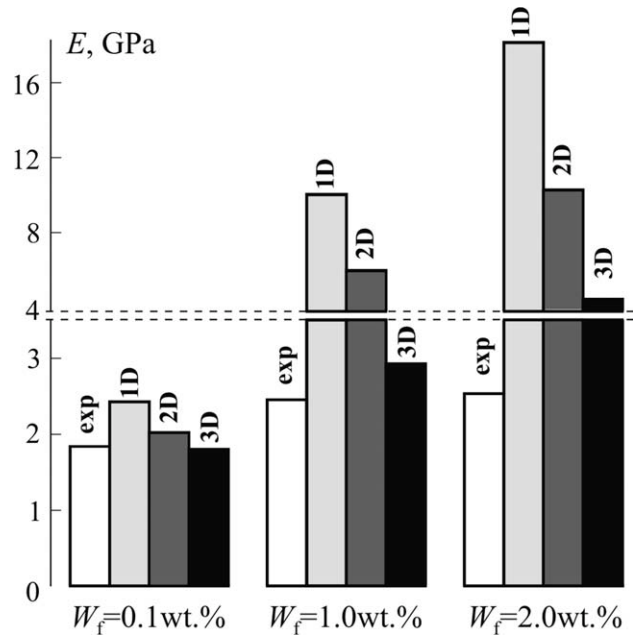


**Figure 3** Experimental data (exp) and theoretical predictions of $E$ of the nanocomposite with the assumption of straight CNTs with different orientations: uniaxially aligned (1D) and randomly oriented in 2D and 3D space.

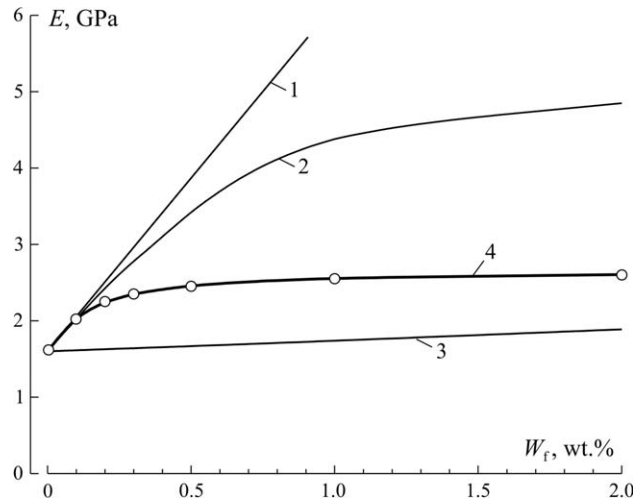


**Figure 4** $E$ as a function of $W_f$ in the composite. Dots indicate experimental data, and lines indicate calculations for the cases of (1) straight CNTs, (2) zigzag-shaped CNTs, (3) totally agglomerated CNTs, and (4) partly agglomerated and curved CNTs.

Poisson's ratio υ of the PVAc were 1.6 GPa and 0.35 accordingly. As one can see, there were great differences between experimentally detected and theoretically predicted values of $E$ of the investigated PVAc/CNT nanocomposites. Also, the theoretical and experimental $E(W_f)$ relationships were different, as shown in Figure 4. By comparing the experimental data with theoretical ones, calculated for the 2D orientation of straight CNTs in a uniform thermoplastic matrix (points and curve 1, respectively), we

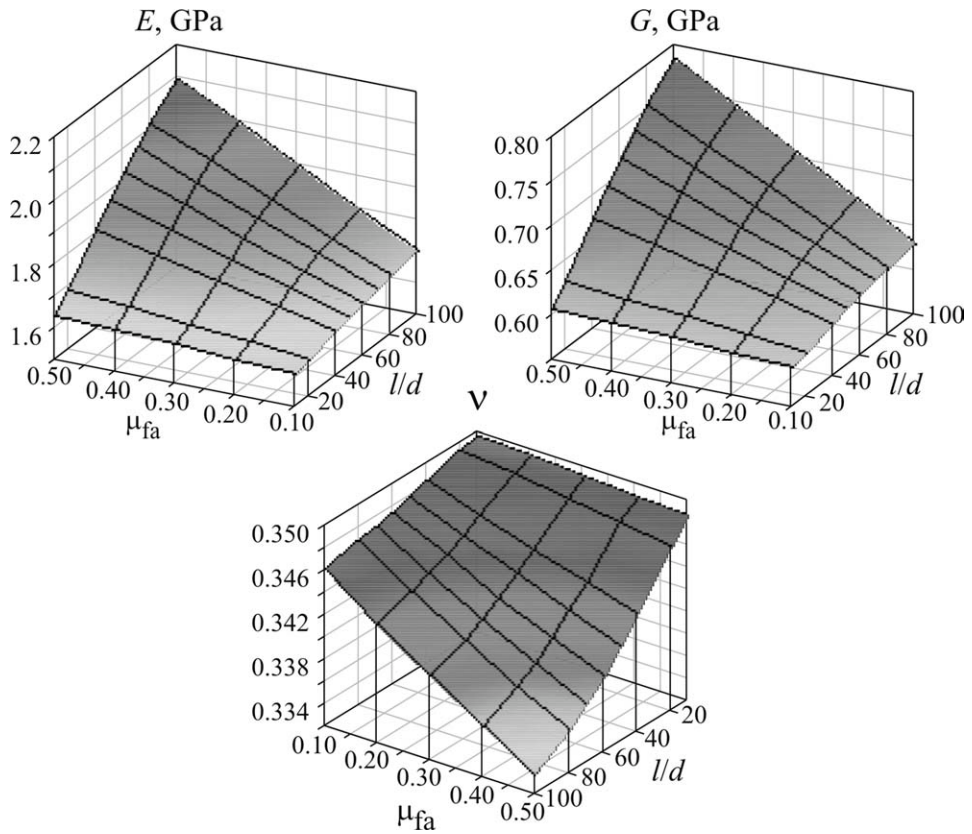


**Figure 5** $E$ of the agglomerates as function of the aspect ratio $l_{fa}/d_f$ and $\mu_{fa}$ of randomly oriented CNTs.

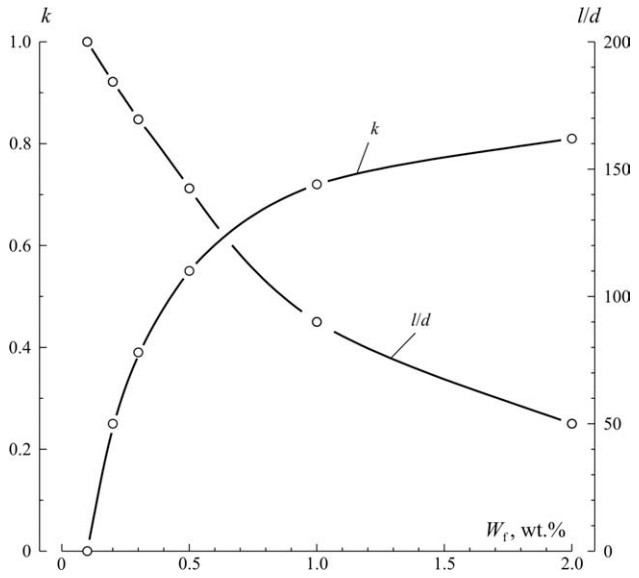


**Figure 6** $k$ and aspect ratio $l_f/d_f$ as functions of $W_f$.

observed a sufficient coincidence only at a low nanofiller content. The most plausible reasons for such behavior were the curvature and agglomeration of the CNTs.

In the calculations, the effect of the curvature was considered by the assumption that in the case of random orientation, CNTs could be represented as zigzags instead of line segments; this led to a decrease of the aspect ratio of CNTs, along with an increasing nanofiller content. As one can see from Figure 4, by comparing theoretically calculated $E$ values in the case of the 2D orientation of curved CNTs (curve 2) with the experimental data points, there were still considerable differences, which were most probably caused by the agglomeration of CNTs.

On the supposition that CNTs are partly agglomerated, let us try to evaluate the degree of agglomeration by introducing the coefficient $k$ ($k = V_{fa}/V_f$, where $V_{fa}$ and $V_f$ represent the agglomerated and total amounts of CNTs in the thermoplastic matrix, respectively). The effective elasticity constants of the inclusions with agglomerated CNTs depend on both the aspect ratio ($l_{fa}/d_f$) of the CNTs and the volumetric part of the nanocomposite ($\mu_{fa}$), containing agglomerated CNTs. With the assumption of a 3D orientation of the agglomerated CNTs in the spherical inclusions, the theoretical values of tensile $E$, calculated for an $l_{fa}/d_f$ range from 10 to 100 and for a $\mu_{fa}$ range from 0.1 to 0.5, are shown in Figure 5. It should be mentioned that the volumetric content of spherical inclusions ($V_a$) with agglomerated CNTs depended on both $V_{fa}$ and $\mu_{fa}$:

$$V_a = V_{fa}/\mu_{fa} = kV_f/\mu_{fa} \quad (3)$$

At small concentrations and total agglomeration, the reinforcing effect of CNT was negligible, as shown in Figure 4, where the straight monotonously growing relationship 3 represents the case when $k = 1$, $\mu_{fa} = 0.2$, and $l_{fa}/d_f = 50$. By comparing experimental data points with the theoretically calculated curve 3, one can assume that in real nanocomposite agglomerations degree of CNTs, characterized by $k$, was changed with the growth of $W_f$. It is clearly demonstrated in Figure 6, where calculated $k$ values of approximation 4, shown in Figure 4 (determined by consideration of the curvature of 2D oriented CNTs with the following structural characteristics of the agglomerates: $\mu_{fa} = 0.2$ and $l_{fa}/d_f = 50$), are depicted as a function of $W_f$.

## CONCLUSIONS

The results of the investigation on the stress–strain characteristics of multiwalled-CNT-modified PVAc nanocomposites testified that along with the increasing weight content of CNT, the modulus of elasticity exponentially increased more than 1.5 times. The growth rate of $E$ of the modulus of elasticity of the PVAc/CNT nanocomposites was highest up to a CNT concentration of 0.5 wt %. At the same CNT concentration $W_f$, $\sigma_y$ and $\sigma_b$ reached maximum values. $\varepsilon_b$ of the investigated nanocomposite, in turn, gradually decreased from more than 500 to 200% with increasing CNT content up to 2 wt %. It was mathematically proven that the elastic constants of CNT-containing polymer nanocomposites depended on both the curvature and agglomeration of the CNTs.

## References

1. Andrews, R.; Weisenberger, M. C. Curr Opin Solid State Mater Sci 2004, 8, 31.
2. Coleman, J. N.; Khan, U.; Blau, W. J.; Gun'ko, Y. K. Carbon 2006, 44, 1624.
3. Ganesan, Y.; Lou, J. JOM 2009, 61, 32.
4. Shaffer, M. S. P.; Windle, A. H. Adv Mater 1999, 11, 937.
5. Xia, H.; Qiu, G.; Wang, Q. J Appl Polym Sci 2006, 100, 3123.
6. Elksnite, I.; Bitenieks, J.; Zicans, J.; Bledzki, A. K. Solid State Phenom 2009, 151, 171.
7. Flandin, L.; Brechet, Y.: Cavaille, J.-Y. Compos Sci Technol 2001, 61, 895.
8. Shi, D.-L.; Feng, X.-Q.; Huang, Y. Y.; Hwang, K.-C.; Gao, H. J. Eng Mater Technol 2004, 126, 250.
9. Odegard, G. M.; Gates, T. S.; Wise, K. E.; Park, C.; Siochi, E. J. Compos Sci Technol 2003, 63, 1671.
10. Brown, J. M.; Anderson, D. P.; Justice, R. S.; Lafdi, K.; Belfor, M.; Strong, K. L.; Schaefer, D. W. Polymer 2005, 46, 10854.
11. Seidel, G. D.; Lagoudas, D. C. Mech Mater 2006, 38, 884.
12. Fiedler, B.; Gojny, F. H.; Wichmann, M. H. G.; Nolte, M. C. M.; Schulte, K. Compos Sci Technol 2006, 66, 3115.
13. Qian, D.; Dickey, E. C.; Andrews, R.; Rantell, T. Appl Phys Lett 2000, 76, 2868.
14. Gorrasi, G.; Sarno, M.; di Bartolomeo, A.; Sannino, D.; Ciambelli, P.; Vittoria, V. J Polym Sci Part B: Polym Phys 2007, 45, 597.
15. Paul, D. R.; Robeson, L. M. Polymer 2008, 49, 3187.

16. Yang, K.; Gu, M.; Guo, Y.; Pan, X.; Mu, G. Carbon 2009, 47, 1723.
17. Nadler, M.; Werner, J.; Mahrholz, T.; Riedel, U.; Hufenbach, W. Compos A 2009, 40, 932.
18. Kanagaraj, S.; Varanda, F. R.; Zhil'tsova, T. V.; Oliveira, M. S. A. Compos Sci Technol 2007, 67, 3071.
19. Thostenson, E. T.; Chou, T. W. J Phys D: Appl Phys 2002, 35, L77.
20. Gorga, R. E.; Cohen, R. E. J Polym Sci Part B: Polym Phys 2004, 42, 2690.
21. Eshelby, J. D. Proc R Soc Ser A 1957, 241, 376.
22. Mori, T.; Tanaka, K. Acta Metall 1973, 21, 571.
23. Plume, E.; Maksimov, R. D.; Lagzdins, A. Mech Compos Mater 2008, 44, 341.
24. Lagzdins, A.; Maksimov, R. D.; Plume, E. Mech Compos Mater 2009, 45, 345.